Journal Title: Nuclear instruments & methods in physics research. Section A, Accelerators, spectrometers, detectors and associated equipment.

Vol. 559, **Is.** 2

Month/Year: April 2006

Pages: 422-425

Article Title: Ullom, Joel; Optimization of transition-edge calorimeter performance

Article Author:

For: Tallmon, Sheila
At: ILL - Boulder Labs Library (CON)

Supplied to you by Baylor University Access Services

OCLC = IYU

BAYLOR UNIVERSITY
UNIVERSITY LIBRARIES

- ☐ Not On Shelf
- ☐ Not As Cited
- ☐ Lack vol/issue
- ☐ Not Yet Received
- ☐ Holdings end before vol/issue
- ☐ Holdings start after vol/issue
- ☐ At Bindery
- ☐ Poor Condition

BU Library Use Only

Group: LVIS
MaxCost: 20IFM
Aging Date: 20100910
*IYU,FGM,MFM,TXM,TTU

Borrowing Notes; @/AM-BCR, LVIS, Nonprofit federal agency. WE DO NOT CHARGE.

Location mymo

Call #

Borrower email:
boulderlabs.ill@noaa.gov

ILL Number: 68858946
[redacted]

Odyssey: 206.107.42.84
[redacted]

Ariel: 140.172.211.165
[redacted]

Ship Via:
Ariel
Document ID (ILL#): 68858946
[redacted]

Patron: Tallmon, Sheila

[redacted]

To (Ariel Address): 140.172.211.165
[redacted]

Ship Via: **Ariel** – To: CON 9/10/2010 5:46 PM **BU OsoFast TN# 422158** [redacted]

Available online at www.sciencedirect.com
SCIENCE DIRECT®
ELSEVIER
Nuclear Instruments and Methods in Physics Research A 559 (2006) 422–425
NUCLEAR INSTRUMENTS & METHODS IN PHYSICS RESEARCH Section A
www.elsevier.com/locate/nima

Optimization of transition-edge calorimeter performance

J.N. Ullom*, J.A. Beall, W.B. Doriese, W.D. Duncan, L. Ferreira, G.C. Hilton, K.D. Irwin, G.C. O'Neil, C.D. Reintsema, L.R. Vale, B.L. Zink

National Institute of Standards and Technology, 325 Broadway, Boulder CO 80305, USA

Available online 11 January 2006

Abstract

Calorimeters that exploit the superconducting-to-normal transition are used to detect individual photons from near-infrared to γ-ray wavelengths. Across this wide range, absorption efficiency, speed, and energy resolution are key performance parameters. Here, we describe recent improvements in the resolution of X-ray and γ-ray transition-edge sensors (TESs). Using the measured dependencies of the high-frequency unexplained noise in TESs, we have optimized the design of our TES X-ray sensors and achieved FWHM energy resolutions of 2.4 eV at 5.9 keV in Constellation-X style sensors and ~2.9 eV at 5.9 keV in larger sensors suitable for materials analysis. We have also achieved a FWHM energy resolution of 42 eV at 103 keV in a TES calorimeter optimized for the detection of hard X-rays and γ-rays.

PACS: 07.20.Fw, 07.85.Fv, 85.25.Am, 95.55.Ka

Keywords: TES; Transition-edge sensor; Microcalorimeter; Unexplained noise

1. Introduction

Transition-edge sensors (TESs) are a promising technology for the detection of single photons from near-infrared to γ-ray wavelengths. These sensors consist of superconducting thin films electrically biased in the resistive transition. The ability of TESs to perform broad-band, high-efficiency, and high-resolution X-ray spectroscopy makes them powerful tools for X-ray astronomy and terrestrial materials analysis. The best energy resolutions obtained so far with X-ray TESs are approximately 4 eV full-width-at-half-maximum (FWHM) at 5.9 keV. Despite this impressive performance, the resolution of TESs has not yet reached the predicted theoretical limits and has shown little improvement in recent years. Given the large range of applications, there is considerable interest in improving sensor performance. For instance, an energy resolution of 2 eV FWHM at 5.9 keV is the goal for the upcoming NASA satellite Constellation-X. Improved energy resolution is also desirable for terrestrial materials analysis since the chemical shifts that distinguish technologically relevant compounds such as Al_2O_3 and SiO_2 from their elemental constituents are $\leqslant 0.5$ eV [1]. Here, we present results from three optimized TES X-ray microcalorimeters. All three sensors perform better than those in previous work, and the best device has an energy resolution of 2.4 ± 0.1 eV FWHM at 5.9 keV. We also present an optimized γ-ray TES with an energy resolution of 42 eV at 103 keV. Sensors with this performance are desirable for applications in astrophysics, nuclear materials analysis, and fundamental physics. For instance, measurement of the 1s Lamb shift in heavy ions with resolution $\leqslant 50$–100 eV can be used to test the predictions of quantum electrodynamics [2].

2. Optimization of X-ray TESs

The energy resolution of a TES microcalorimeter depends on its transition temperature T_c, heat capacity C, and the sharpness of the superconducting-to-normal transition, described by the parameter $\alpha = (T/R)\ \mathrm{d}R/\mathrm{d}T$ where R is the sensor resistance. For simplicity, we take $\beta = (I/R)\ \partial R/\partial I$ to be zero, although this quantity is

*Corresponding author. Tel.: +1 303 497 4408; fax: +1 303 497 3042.
E-mail address: ullom@boulder.nist.gov (J.N. Ullom).

0168-9002/$ - see front matter © 2006 Elsevier B.V. All rights reserved.
doi:10.1016/j.nima.2005.12.173

known to be finite. We have modified the traditional expression for the resolution of a TES [3] to include finite bath temperatures and finite loop gain. In addition, we include degradation by unexplained noise (UN): noise not accounted for by either the Johnson noise or thermodynamic fluctuations in the device thermal conductances. The UN is treated as a white voltage noise whose magnitude M is expressed as a fraction of the zero-inductance high-frequency limit of the Johnson noise. The spectral density of the resulting noise current is $M\sqrt{4k_bT_c/R}\,\mathrm{A}/\sqrt{\mathrm{Hz}}$, where $R = V/I$. Assuming a stiff voltage bias, the FWHM energy resolution is

$$\Delta E_{\mathrm{FWHM}} = 2.355\sqrt{\frac{4k_bT_c^2Cn(1+M^2)}{\alpha^2(1-t^n)}}\sqrt{1+\frac{\alpha^2(1-t^n)F}{n(1+M^2)}},$$

where n is the exponent governing power flow between the TES and the heat bath (typically 3–5), $t = T_b/T_c$ is the ratio of the bath and transition temperatures, and F depends on the nature of energy transport between the TES and the bath. Recent measurements indicate that TES calorimeters on unpatterned SiN_x membranes are in the specular limit [4] for which $F = (1+t^{n+1})/2$ [5]. In the common limits $T_b \ll T_c$ and $\alpha^2/(1+M^2) \gg 2n$, we find $\Delta E_{\mathrm{FWHM}} = 2.355\sqrt{4k_bT_c^2Cn/\alpha}\sqrt{(1+M^2)n/2}$. It can readily be seen that sensor performance is improved by lowering T_c and C. The narrow temperature range over which the TES resistance responds to temperature imposes an additional constraint on C and α: namely, the device must retain temperature sensitivity during the temperature excursion $\Delta T = E_\gamma/C$ produced by the absorption of a photon with energy E_γ. Furthermore, because of the inverse relation between signal current and device resistance, the response of a TES to deposited energy becomes nonlinear well before the device is fully saturated (driven normal). While some nonlinearity is acceptable, excessive nonlinearity degrades the energy resolution. The maximum photon energy $E_{\gamma-\max}$ that a sensor can measure without degraded performance will be proportional to C/α since α is inversely proportional to the temperature width of the transition. We define $E_{\gamma-\max}$ to be $0.8\ CT_c/\alpha$, where α is evaluated in the small-signal limit at $R/R_N = 0.25$ [6]. This expression is only an approximation; however, it provides a good measure for comparing devices.

We next describe two strategies for optimizing the energy resolution of a TES microcalorimeter. These strategies build on Ref. [7], in which we found that the magnitude of the UN increases with α. For the conditions in [7], $M \sim 0.2\alpha^{1/2}$. In addition, we found that α could be controllably suppressed from intrinsic values greater than 500 to as low as 10 by the application of a perpendicular magnetic field or by incorporating normal-metal regions into the TES perpendicular the direction of current flow. We consider first the case where the TES heat capacity is fixed. This constraint arises if system requirements such as collecting area dictate the pixel size. Substituting the expression for M into ΔE, sensor performance is maximized by maximizing α, even though the UN is increased. Hence, when C is fixed, α should be increased until $E_{\gamma-\max}$ is matched to the peak photon energy of interest. We consider second the case where C can be treated as a free parameter. Here, it is desirable to simultaneously reduce C and α while keeping the ratio C/α constant so that $E_{\gamma-\max}$ is matched to the peak photon energy of interest. The low value of α reduces the UN and improves the energy resolution.

To demonstrate these optimization strategies, we fabricated three X-ray TESs with transition temperatures near 115 mK. The devices consisted of bilayers of Mo and Cu with a 1.5 μm Bi absorber. The devices are suspended on a 0.4 μm Si_3N_4 membrane. The devices were fabricated using our standard process, which includes an additional Cu layer for edge passivation and the normal metal features that suppress α. The normal-state resistance of the devices was ~11 mΩ. The devices were operated at bath temperatures of 60–70 mK. A solenoid was used to control the magnetic field perpendicular to the plane of the devices, and 5.9 keV X-rays were supplied by a ^{55}Fe source. The devices were operated with a voltage bias and the signal currents were measured with a SQUID ammeter.

Device designs fall on the C–α plane shown in Fig. 1. Lines through the origin correspond to a constant $E_{\gamma-\max}$. Methods used to determine C and α are given in Ref. [6]. Device A was 400 μm on a side and had six perpendicular normal bars to reduce α and M. Previous devices with these dimensions but without the bars had an energy resolution of 4.5 eV. The best resolution obtained with device A was 3.2 eV when the perpendicular field was zero and α was the highest. However, even in zero field, device A was far from saturation; device A lies on the line for $E_{\gamma-\max} = 20.6$ keV. To test optimization strategy 1, we fabricated device B which was also 400 μm on a side and had only three normal bars to increase α and better match $E_{\gamma-\max}$ to 5.9 keV. Since the bars make only a small contribution to the heat capacity, this change corresponds to horizontal motion to

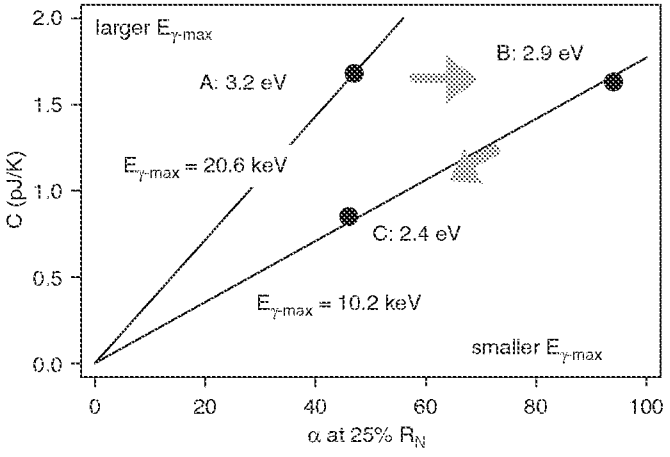

Fig. 1. Parameter space for X-ray TES design.

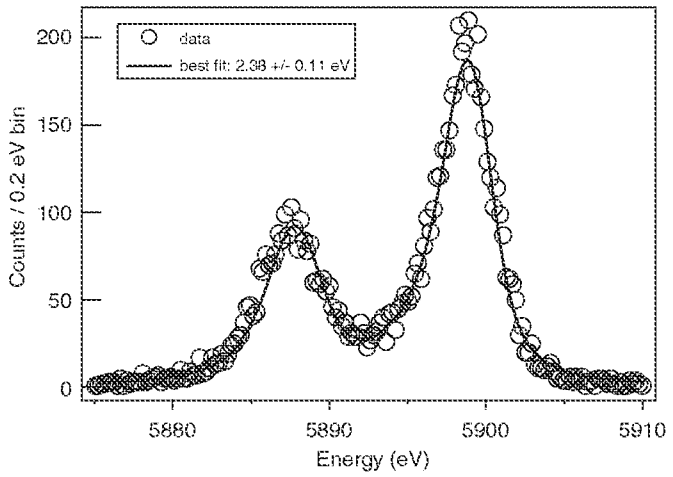

Fig. 2. Fe-55 spectrum showing 2.38 eV resolution at 5.9 keV. The displayed region of the histogram contains 7754 counts obtained over 3700 s.

the right in Fig. 1. $E_{\gamma-\max}$ of device B was close to 10.2 keV and the energy resolution improved to 2.9 eV. To test optimization strategy 2, we fabricated device C, which was 250 μm on a side and had five normal bars. Because of its smaller size, the heat capacity of device C was roughly half the heat capacity of device B (and A). The change from three to five bars reduced α by a similar factor, thus maintaining $E_{\gamma-\max}$ near 10.2 keV. Hence, the change from B to C corresponds to motion towards the origin of Fig. 1 along the line corresponding to $E_{\gamma-\max} = 10.2$ keV. For both devices B and C, best results were achieved using a small magnetic field to broaden the transition. Device C had the lowest α, the lowest M, and the best resolution of the three devices. As shown in Fig. 2, the resolution of device C was 2.4 eV at 5.9 keV.

3. Optimization of γ-ray TESs

Using similar design strategies to those described above, we have fabricated γ-ray TES calorimeters with resolution better than previous work. Since thin films lack the stopping power required for γ-rays, our sensors consist of a Mo/Cu bilayer thermometer and a bulk Sn superconducting absorber. The absorber has dimensions 0.9 mm × 0.9 mm × 0.25 mm and is glued to the thermometer. As shown in Fig. 3, we measured a resolution of 42 eV FWHM at 103 keV in a sensor with a thermal response time of 1.2 ms.

The fabrication of arrays of 10^2 or more elements is challenging because of the need for array-compatible absorber attachment techniques. We have devised and tested techniques to attach bulk absorbers across a TES array. First, all the absorbers necessary for an array are positioned in a micromachined carrier. Identical portions of glue are applied simultaneously across the TES array and then the TESs and absorbers are mated. Using these techniques, we have successfully fabricated 9-pixel mechanical test structures.

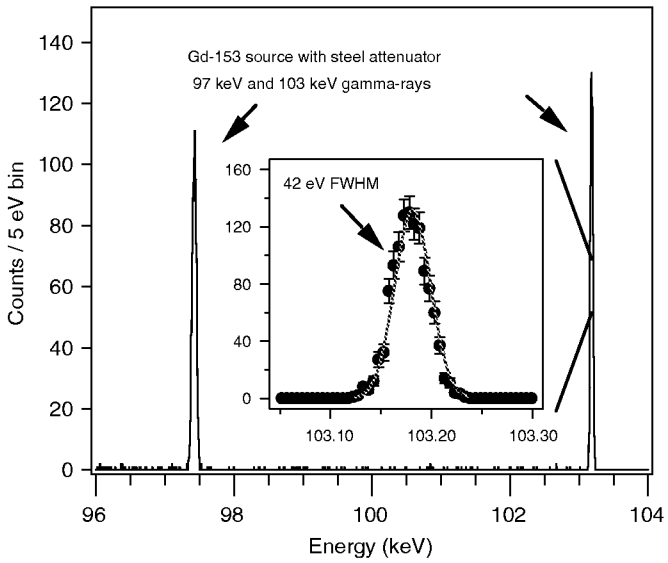

Fig. 3. Gd-153 spectrum showing 42 eV resolution at 103 keV.

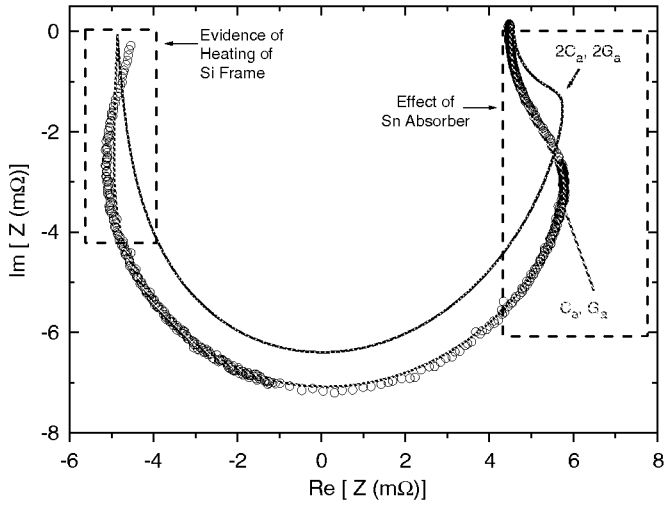

Fig. 4. Real and imaginary components of the electrical impedance of a γ-ray TES detector. Each point corresponds to a different frequency. Theory is shown for two values of the heat capacity C_a of the absorber and the conductance G_a between the TES and absorber. While C_a/G_a is preserved, only one theory curve fits the data.

To compare and optimize γ-ray TESs, it is desirable to understand their complex thermal circuit. As shown in Fig. 4, measurements of the frequency-dependent impedance can be used to determine important detector parameters such as the heat capacity of the absorber and the thermal conductance between the absorber and thermometer [8,9].

4. Conclusions

We have demonstrated techniques for optimizing the energy resolution of X-ray and γ-ray TESs. We have also demonstrated techniques for fabricating arrays

of γ-ray TESs and for characterizing their complex thermal circuit. Further improvements in sensor resolution are expected.

Acknowledgement

We acknowledge the assistance of Marcel van den Berg and support from NASA's Constellation-X program and Grant NDPR S06561-G.

References

[1] S.W. Nam, et al., Microscop. Microanal. 7 (Suppl. 2: Proc.) (2001) 1050.
[2] A. Bleile, et al., in: AIP Conference Proceedings 605, Low Temperature Detectors, 2001.
[3] K.D. Irwin, Appl. Phys. Lett. 66 (1995) 1998.
[4] H.F.C. Hoevers, et al., Appl. Phys. Lett. 81 (2005) 251903.
[5] W.S. Boyle, K.F. Rodgers, J. Opt. Soc. Am. 49 (1959) 66.
[6] J.N. Ullom, et al., Appl. Phys. Lett. 87 (2005) 194103.
[7] J.N. Ullom, et al., Appl. Phys. Lett. 84 (2004) 4206.
[8] M.A. Lindeman, et al., Rev. Sci. Instr. 75 (2004) 1283.
[9] M. Galeazzi, et al., J. Appl. Phys. 93 (2003) 4856.